FULL PAPER

Dalton
www.rsc.org/dalton

Molecular mechanics for multiple spin states of transition metal complexes †

Robert J. Deeth,* David L. Foulis and Benjamin J. Williams-Hubbard
Inorganic Computational Chemistry Group, Department of Chemistry, University of Warwick, Coventry, UK CV4 7AL. E-mail: r.j.deeth@warwick.ac.uk; http://www.chem.warwick.ac.uk/iccg

Received 27th May 2003, Accepted 28th August 2003
First published as an Advance Article on the web 10th September 2003

Empirical Ligand Field Molecular Mechanics (LFMM) parameters for Co^{III}–F and Co^{III}–CN bonds are developed from Density Functional Theory (DFT) calculations on octahedral $[CoF_6]^{3-}$ and $[Co(CN)_6]^{3-}$. In addition to the $^5T_{2g}$ and $^1A_{1g}$ ground states of $[CoF_6]^{3-}$ and $[Co(CN)_6]^{3-}$ respectively, DFT can also access the low-spin form of $[CoF_6]^{3-}$ and the high-spin form of $[Co(CN)_6]^{3-}$ as well as the averaged d configuration (ADC) state corresponding to a $t_{2g}^{3.6}e_g^{2.4}$ configuration in which the ligand field stabilisation energy is formally zero. DFT orbital energies are used to estimate the dependence of Δ_{oct} on the Co–L distance which, when used in conjunction with the relation that the DFT spin state energy difference $\Delta E_{spin}(^5T_{2g}–^1A_{1g}) = 2\Delta_{oct} - (5B + 8C)$, provides a measure of the interelectron repulsion energy. Finally, the ratio of e_σ to e_π ligand field parameters is obtained *via* fitting the DFT orbital energies of hypothetical square planar $[CoF_4]^-$ and $[Co(CN)_4]^-$ complexes using an ADC corresponding to a $b_{1g}^{1.2}b_{2g}^{1.2}a_{1g}^{1.2}e_g^{2.4}$ configuration. The LFMM parameters are derived solely from the homoleptic systems but are nevertheless able to reproduce the structures and spin-state energies of the eight mixed-ligand systems in between. The latter are estimated theoretically since no experimental data exist. The high-spin and low-spin structures have Co–L rms errors of 0.06 and 0.03 Å, respectively. Explicit recognition of d–d interelectron repulsion energies provides a common reference for both spin states which facilitates a direct LFMM calculation of the spin-state energy difference. Both LFMM and DFT predict: (i) a change from high to low spin after replacement of a single fluoride ligand; (ii) the difference increases with each subsequent replacement and (iii) $^1A_{1g}$ is relatively more stable than $^5T_{2g}$ for *cis* and *mer* compared to *trans* and *fac*, respectively. The spin-state energy difference rms error is ~7 kcal mol^{-1} but there is a systematic overestimation for the mixed-ligand systems since the LFMM does not fully capture the *cis* and *trans* influences.

Introduction

Molecular mechanics (MM) is a popular technique for modelling the molecular structures of organic systems and biomolecules.[1–3] However, the extension of conventional MM to systems containing open-shell, d^n transition metal centres presents new challenges.[4–8] The structural and energetic effects arising from the incomplete d shell can be profound.[9] For example, high-spin d^8 Ni(II) complexes usually possess six-coordinate octahedral geometries while their low-spin counterparts are invariably square planar and with significantly shorter Ni–L bond lengths. To account for the bond length change within conventional MM requires two independent sets of force field (FF) parameters, one tuned for high-spin and one for low-spin species.[7] However, since the different FF parameter sets result in different references states, the high-spin and low-spin strain energies cannot be directly compared and MM cannot address the general question of which spin state would have the lowest overall energy. This behaviour contrasts with quantum-mechanical methods which do yield a common reference state and can predict the lowest energy, assuming a correct and suitably accurate treatment of spin states.

From a coordination chemistry perspective, the difference between high- and low-spin Ni(II) complexes, for example, is due to the changes in the d orbital occupations and the structural changes can be readily interpreted in terms of variations in the ligand field stabilisation energy (LFSE). We are developing an augmented form of MM which explicitly calculates the LFSE *via* a generalised ligand field theory (LFT) term in the MM strain energy expression.[5] Using this 'hybrid' ligand field/molecular mechanics (LFMM) approach for Ni(II) amine systems, a *single* set of FF parameters has been developed which simultaneously models the *structures* of both high- and low-spin systems.[10] However, both the LFMM and conventional MM approaches have not yet addressed how to compare the *energies* in different spin states.

LFT tells us that the spin state is a balance between the one-electron energy – *i.e.* the LFSE – and a two-electron term – *i.e.* the d–d interelectron repulsion. The LFSE favours low-spin configurations while interelectron repulsion favours high-spin states. The final observed spin state is thus a competition between these two factors. Thus, one way to model the spin state correctly would be to carry out the LFT calculation within the full many-electron basis.

Assuming that Russell–Saunders coupling is valid and that spin–orbit effects can be ignored, the orbitally five-fold degenerate one-electron LFSE calculation, which applies rigorously only to d^1/d^9 configurations, would be replaced by a 25-fold, 50-fold, 104-fold or 100-fold problem for d^2/d^8, d^3/d^7, d^4/d^6 or d^5, respectively. Not only does this represent a substantial increase over the simple one-electron case but the mathematical complexity of extending the analytical expressions for the one-electron energy derivatives[11] to a many electron basis is daunting.

An alternative procedure is to derive the electrostatic energy correction from another source, either based on experiment or theory. Providing the d–d interelectron repulsion energies are correctly balanced with respect to the LFSE, a common reference energy will be established for all spin states and a direct comparison of the total energies will be possible.

This paper describes a strategy for defining a common reference energy for LFMM-based calculations on TM systems which will facilitate the direct prediction of the most favourable spin state. As a 'proof of concept', we have chosen the d^6 Co(III) complexes $[CoF_6]^{3-}$ and $[Co(CN)_6]^{3-}$ to develop LFMM

† Electronic supplementary information (ESI) available: Fig. S1: Inverse power series fit of Δ_{oct} against bond length for $[CoF_6]^{3-}$. Comparison of DFT and LFMM structures. See http://www.rsc.org/suppdata/dt/b3/b305868a/

DOI: 10.1039/b305868a

parameters which will be then be applied directly to the predictions of the structures and spin-state energies of all the intervening mixed-ligand systems. Since there are no experimental data for the mixed-ligand complexes, the entire exercise has to be based on theoretical calculations, although these are initially validated on the homoleptic complexes. The aim is to explore whether the LFMM approach based solely on data for the homoleptic systems will faithfully reproduce the structures and energies of the mixed-ligand systems without further modification of the parameters.

Computational details

The DFT calculations were obtained using the Amsterdam Density Functional (ADF) program versions 2.3[12] and 2000.02.[13] STO basis sets of triple-ζ + polarisation quality were used on all atoms with frozen cores[14] up to 2p on Co and 1s on F, C and N. Unless otherwise stated, geometries were optimised *in vacuo* using default convergence criteria and either the local density approximation (LDA)[15] with the Vosko–Wilk–Nusair correlation term[16] or its gradient corrected version with the Becke88 exchange[17] and Perdew86[18,19] correlation expressions. Environmental effects were included using the COSMO model implemented in ADF2000 with parameters appropriate to aqueous solution at 293 K. Rigorous point group symmetry was applied as detailed in the text and tables.

LFMM results were obtained using our in-house FORTRAN code DOMMINO version 3.0. Geometries were obtained using analytical energy gradients with a convergence criterion of 0.01 kcal mol^{-1}.

Ligand field calculations used the CAMMAG program[20] with basis sets and parameters as described in the text.

Results and discussion

The low-spin octahedral t_{2g}^6 configuration yields a non-degenerate $^1A_{1g}$ ground state and corresponds to the lowest LFSE for this symmetry. The high-spin $t_{2g}^4e_g^2$ configuration generates a $^5T_{2g}$ ground term which is formally Jahn–Teller active but since the Jahn–Teller instability refers to π-type t_{2g} orbitals, relatively small distortions are expected. Thus, d^6 complexes will be basically octahedrally coordinated in both high- and low-spin states. Furthermore, under octahedral symmetry, the intermediate triplet spin state cannot become the ground state and is not considered here.

The goal of the present study is to use only the homoleptic complexes MA_6 and MB_6 as a basis for deriving a single set of LFMM parameters which will correctly predict the structures and relative spin-state energies for the mixed-ligand species MA_nB_{6-n}. MA_6 is chosen to be high spin while MB_6 is a low-spin complex. The LFMM prediction of the value of *n* at which the spin state changes can be tested against experiment and/or theory. To our knowledge, there is only one high-spin homoleptic complex of Co(III), $[CoF_6]^{3-}$. Since we are not yet concerned here with modelling environmental effects such as solvation, the overall complex charge needs to be kept constant in order to exploit the law of average environment. $[Co(CN)_6]^{3-}$ was chosen as a suitable low-spin example.

$[CoF_6]^{3-}$

In order to develop LFMM parameters for a given complex it is necessary to have structural and energetic data for each spin state. Only one spin state will correspond to the ground state but experimental electronic spectra and/or theoretical methods like ligand field theory (LFT) and density functional theory (DFT) can be employed to fill in the gaps. Under O_h symmetry, the LFMM parameters can be based on analytical expressions. Accordingly, the initial set of DFT calculations imposed rigorous octahedral symmetry.

The Co–F distance in K_3CoF_6 crystals is 1.89 Å and the calculated *in vacuo* bond lengths for the $^5T_{2g}$ state are 1.97 Å using the LDA and 2.03 Å for the BP86 functional. As is typical for this type of anionic Werner complex, the gradient corrected functional gives M–L bonds which are too long while the simpler LDA does rather better.[21] However, the apparently superior performance of the LDA is something of a happy accident.

The energy levels from *in vacuo* quantum mechanical calculations on anionic systems are elevated which can generate one or more occupied orbitals with positive energies. This is physically unreasonable as the electrons are formally unbound. However, the finite extent of the atomic basis functions prevents the electrons from dissociating completely. Nevertheless, they tend to occupy as diffuse functions as possible which affects the metal–ligand bonding. To the extent that the nominally more accurate gradient-corrected functionals generate longer bonds, one could propose that the unbound electrons tend to weaken the bonds. However, the overbinding typical of the LDA is partially compensating for this and the gas-phase LDA geometry happens to correspond better to the experimental condensed-phase value.

Embedding the complex in a condensed phase lowers the orbital energies and stabilises the system and the M–L bond lengths would be expected to shorten. Within ADF, environmental effects can be treated using the COSMO solvation model. With parameters appropriate to aqueous solution plus atomic radii of 2.36 and 1.68 Å for Co and F, respectively – *i.e.* 20% larger than their van der Waals radii – the calculated Co–F distance using the BP86 functional is shortened by around 0.1 to 1.96 Å, a value which is 0.07 Å longer than the crystal structure value but very close to the *in vacuo* LDA value. Hence, for whatever reason, *in vacuo* LDA calculations predict reasonable structures and are quick and easy to execute. We will assume that the errors are relatively constant and use the LDA to compute both the high-spin ground state and the hypothetical low-spin state for $[CoF_6]^{3-}$. The latter is 1.88 Å corresponding to a 0.09 Å shortening, consistent with the enhanced LFSE of the $^1A_{1g}$ state.

However, the LDA *energies* cannot be used directly since the $^1A_{1g}$ LDA energy is 3 kcal mol^{-1} *lower* than $^5T_{2g}$. This is not wholly unexpected. Studies on related $[MX_6]^{2-}$ complexes have shown[21] that gradient corrected functionals such as BP86 give superior energies to the LDA and indeed, the BP86 energies computed at the high- and low-spin optimised LDA geometries re-establish $^5T_{2g}$ as the lower energy state by 3.1 kcal mol^{-1} but, as shown in Fig. 1, the vertical energy difference is still incorrect. The double headed arrows connect the optimised low-spin (open triangles) to its corresponding optimised high-spin counterpart (filled squares). However, if one computes at the

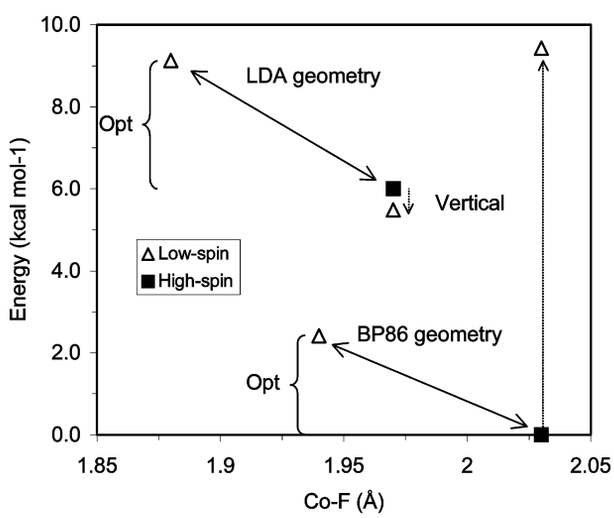

Fig. 1 BP86 energies for $[CoF_6]^{3-}$ at various Co–F distances.

high-spin LDA geometry (1.97 Å) the BP86 energy of the low-spin state, this comes out about 0.5 kcal mol^{-1} below $^5T_{2g}$ as indicated by the short downward pointing arrow in Fig. 1. This arises since the LDA *structure* is not a stationary point on the BP86 *energy surface*. Including the environment does not solve the problem as the BP86/COSMO method predicts that $[CoF_6]^{3-}$ should be low spin at all Co–F distances.

The correct energy behaviour is recovered if the BP86 functional is employed for everything. The spin-state energy difference using BP86 optimised structures (2.5 kcal mol^{-1}) is indicated by the double-headed arrow in the lower part of Fig. 1 and is similar to the LDA-structure value (3.1 kcal mol^{-1}). However, now the vertical $^5T_{2g} \longrightarrow {}^1A_{1g}$ energy difference at the high-spin geometry is in the correct sense with a value of 9.1 kcal mol^{-1}. Some insight as to whether this energy difference is reasonable can be gained from Ligand Field calculations.

The $^5T_{2g} \longrightarrow {}^1A_{1g}$ transition is not observed experimentally and the ^5E_g excited state is subject to a strong Jahn–Teller effect and two spin-allowed 'd–d' absorptions are observed. Nevertheless, the spectra of $[CoF_6]^{3-}$ species have been analysed using LFT on the basis of octahedral symmetry. Figgis quotes Δ_{oct} = 13100 cm^{-1} and B = 787 cm^{-1},[22] while Allen *et al.*[23] favour Δ_{oct} = 14100 cm^{-1}, B = 765 cm^{-1} and C = 3672 cm^{-1}

The former data imply a nephelauxetic reduction of 0.73 relative to the Co^{3+} free-ion value (B_0 = 1080 cm^{-1}). In the absence of spin–orbit coupling, the quintet–singlet splitting can be computed from a ligand field calculation which employs only the spin-quintet and spin-singlet free ion terms. Accordingly, the basis set comprised ^{5} D, ^{1}I, ^{1}G(1), ^{1}G(2), ^{1}F, ^{1}S(1), ^{1}S(2) ^{1}D(1) and ^{1}D(2). Taking Δ_{oct} to be 13100 cm^{-1} and B = 787 cm^{-1}, C was adjusted until the $^5T_{2g}$–$^1A_{1g}$ splitting, ΔE_{q-s}, equalled the DFT estimate of ~3200 cm^{-1} (*i.e.* 9.1 kcal mol^{-1}). For C = 3217 cm^{-1}, the splitting is 3425 cm^{-1}. This corresponds to a C/B ratio of 4.1 and a nephelauxetic reduction of 0.63 for C. Both results are consistent with ligand-field expectations[22] in that C/B is usually around 4 and similar nephelauxetic effects are expected (but not required) for both interelectron repulsion parameters. Moreover, a full-basis LFT calculation places the first excited triplet state at 6669 cm^{-1} which correlates with a band observed at 5500 cm^{-1}. However, the spin-state splitting is quite sensitive both to C/B and to Δ_{oct}. Changing the former to 4.0 increases ΔE_{q-s} by ~500 cm^{-1} while decreasing the latter to 12500 cm^{-1} increases ΔE_{q-s} by ~1100 cm^{-1}.

The second set of ligand field parameters places the $^1A_{1g}$ level 4924 cm^{-1} (14.1 kcal mol^{-1}) above the ground state which is in modest agreement with the vertical BP86 energy difference of 3193 cm^{-1}.

Overall, the BP86 $^5T_{2g} \longrightarrow {}^1A_{1g}$ energy difference of 9.1 kcal mol^{-1} at the BP86-optimised geometry is consistent with LFT estimates. Averaged CASSCF coupled pair functional calculations[24] for $[CoF_6]^{3-}$ embedded in a Madelung potential appropriate to K_3CoF_6 place this transition between 3380 and 5580 cm^{-1} depending on the size of the active space. The larger active space gave the lower transition energy. In summary, therefore, the current BP86 estimates of the relative spin state energies of $[CoF_6]^{3-}$ appear adequate but since the BP86 geometry is not as good as the LDA structure, the LFMM parameterisation is based on LDA optimised geometries but BP86 energies at the BP86 geometries. In effect, this corresponds to shifting the BP86 energy curve until the high-spin minimum corresponds to the LDA optimised bond length, a reduction of ~0.06 Å for $[CoF_6]^{3-}$. We then take the first excited spin singlet state as 9.1 kcal mol^{-1} above the ground spin quintet. Paradoxically, then, the LFMM can be designed to give better agreement with experiment than DFT on its own.

Another important piece of structural data concerns what the Co–F distance would be in the absence of any LFSE contribution. This corresponds to the value that the LFMM model should deliver from just the conventional MM energy terms alone (*vide infra*). Again, DFT proves extremely useful. The LFSE is zero when all five d orbitals have identical populations. For a d^6 octahedral complex, this corresponds to a $t_{2g}^{3.6}e_g^{2.4}$ configuration with each individual d orbital containing 1.2 electrons. Since DFT depends on the electron density, there is no formal requirement that orbitals must contain a whole number of electrons.[25] Hence, the DFT calculation for this 'averaged d configuration' (ADC) remains valid. However, the ADC will only be an approximation to the zero-LFSE state because of differential covalency effects. The σ-bonding e_g molecular orbitals will be more delocalised than the π-type t_{2g} set so that the contributions to the σ-type d orbital populations will be less than their π-type counterparts. The LDA-optimised Co–F distance for the ADC is 1.99 Å, that is about 0.02 Å longer than the high-spin value, consistent with the loss of $-2/5\Delta_{oct}$ stabilisation energy.

Having tested the DFT procedures, we assume that the calculated relative spin state energies for different Co–F distances remain reliable. The resulting curves can then be put on an absolute scale by expressing the ADF binding energies relative to an isolated Co^{3+} cation with six F^- anions. The binding energies are large, reflecting the dominant electrostatic contributions but since the total energies are explicitly separated from the treatment of the spin-state energy differences, errors in the former do not influence the latter.

Fig. 2 shows the resulting energy curves for $[CoF_6]^{3-}$. The DFT calculations also provide estimates for Δ_{oct} as a function of Co–F bond length and since for a d^6 system, the quintet–singlet spin crossover point occurs for $2\Delta_{oct} = 5B + 8C$, the spin-state energy difference also provides an estimate of the interelectron repulsion energy as a function of Co–F distance and hence the basis for a direct comparison of LFMM spin state energies.

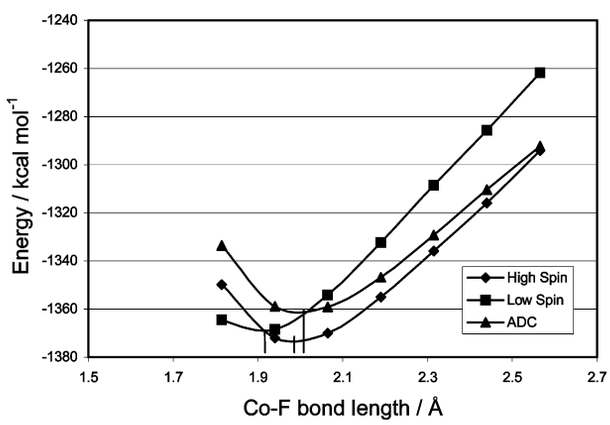

Fig. 2 Bond length *versus* energy for various electronic configurations of $[CoF_6]^{3-}$.

As described previously, the LFMM strain energy expression combines the terms of conventional MM with a d-electron stabilisation energy term computed *via* generalised ligand field theory. For a simple complex like $[CoF_6]^{3-}$, the LFMM strain energy expression comprises only four terms, ΣE_{str}, ΣE_{nb}, E_{LFSE} and E_{spin} where the summations extend over all appropriate interactions. A Morse function is used for the bond stretch energy, E_{str}, to facilitate modelling large bond length variations (eqn. (1)). D is the well depth, r_0 the ideal bond length and a relates to the curvature.

$$E_{str} = D[1 - \exp(-a(r - r_0))]^2 - D \qquad (1)$$

The non-bonding interactions, ΣE_{nb}, have a van der Waals component, ΣE_{vdw}, as well as an optional electrostatic component, ΣE_{el}. The latter is not included in the present work. The van der Waals interactions are modelled by a 6–9 potential of the form shown in eqn. (2).

Table 1 Calculated Co–F distances and relative binding energies for $[CoF_6]^{3-}$. Column 2 refers to which functional was used to optimise the bond length

State	Geometry	Co–F/Å	E(BP86)/kcal mol^{-1}
$^5T_{2g}$	LDA	1.97	−613.0
$^1A_{1g}$	LDA	1.88	−609.8
$^5T_{2g}$	BP86	2.03	−619.0
$^1A_{1g}$	BP86	1.94	−616.6
$^1A_{1g}$	Fixed	1.97	−613.5
$^1A_{1g}$	Fixed	2.03	−609.9

$$E_{vdw} = A/r^9 - B/r^6 \quad (2)$$

In eqn. (2), r is the distance between the interacting centres and A and B are constants. In the LFMM method, ligand–ligand non-bonded interactions are allowed hence the absence of an explicit angle bend term. However, E_{vdw} for the metal–ligand bond is subsumed within the bond stretch term and no explicit Co–F van der Waals is considered. That is, A and B for the metal are set to zero. Together, the bond stretch and van der Waals term describe the complex in the absence of any d electron stabilisation energy and can thus be compared directly to the DFT ADC energy curve. This provides the separation between the treatment of total energies and the spin-state energy differences mentioned above.

In the cellular ligand field (CLF) model or equivalently the angular overlap model (AOM), Δ_{oct} is expressed in terms of local energy parameters describing the separate metal–ligand σ and π bonds, e_σ and e_π, respectively. For an octahedral d^6 complex, the ligand field stabilisation energy (LFSE) is a simple function of the CLF/AOM parameters as shown in eqns. (3), (4) and (5).

$$E_{LFSE}(\text{high spin}) = -2/5\Delta_{oct} \quad (3)$$

$$= -2/5(3e_\sigma - 4e_\pi) \quad (4)$$

$$E_{LFSE}(\text{low spin}) = -12/5(3e_\sigma - 4e_\pi) \quad (5)$$

To be of use in the LFMM model, the parameters must be expressed as functions of the geometry. Angular contributions are implicitly accounted for so all that is required is to express e_σ and e_π as functions of the metal–ligand bond length. Unfortunately, the octahedral d-orbital splitting only yields one degree of freedom, namely Δ_{oct}. We therefore proceed in three stages.

Firstly, the Δ_{oct} values from the DFT calculations were fitted to an inverse power series, *i.e.* $\Delta_{oct} = Kr^{-N}$. An r^{-4} dependence reproduces the DFT curve quite well (see Fig. S1 in the ESI †) and compares reasonably well with the r^{-5} behaviour predicted by the electrostatic crystal field theory. As noted elsewhere,[10] a linear bond length dependence is also a fair approximation especially in the present case where Co–F distances do not vary widely.

Secondly, analytical expressions for each term of the LFMM energy were derived and the values of D, r_0 and a adjusted to provide the best fit with all the DFT data (Table 1). The value of r_0 was then compared to the ideal Co–F distance for the ADC. The two were found to be in close agreement (1.98 and 1.99 Å, respectively).

Thirdly, a protocol was developed to estimate the ratio of e_π to e_σ. For a hypothetical planar $[CoF_4]^-$ complex with D_{4h} symmetry, the d-orbital splittings are simple functions of e_σ, e_π and the d–s mixing parameter, e_{ds}:

$$\Delta E(d_{x^2-y^2} - d_{xy}) = 3e_\sigma - 4e_\pi \quad (6a)$$

$$\Delta E(d_{x^2-y^2} - d_{xz}/d_{yx}) = 3e_\sigma - 2e_\pi \quad (6b)$$

$$\Delta E(d_{x^2-y^2} - d_{z^2}) = 2e_\sigma + 4e_{ds} \quad (6c)$$

Table 2 LFMM parameters for $[CoF_6]^{3-}$ (σ-bonding only) and optimised LFMM bond lengths (Å) and total energies (kcal mol^{-1}). DFT values in italics. D, r_0 and a refer to the Morse funtion, $\Delta_{oct} = K/r^N$, A and B are the van der Waals parameters and $5B + 8C$ models the d–d interelectron repulsion energy added to the low-spin state

D/kcal mol^{-1}	227.1
r_0/Å	1.98
a	0.70
N	4
K/kcal mol^{-1}	398.1
A/kcal mol^{-1} Å^{-9}	7240
B/kcal mol^{-1} Å^{-6}	320
$(5B + 8C)$/kcal mol^{-1}	$-33.13r^2 + 112.77r - 27.46$
Co–F high spin/Å	1.97; *1.97*
Total energy, high spin/kcal mol^{-1}	−1372.9; *−1373.0*
Co–F low spin/Å	1.89; *1.88*
Total energy, low spin/kcal mol^{-1}	−1369.9; *−1369.8*

A DFT calculation with Co–F distances set at 1.97 Å can be used to estimate the d orbital energies. However, in order to make better contact with LFT, care must be taken to remove the effects of d–d interelectron repulsions in the DFT. LFT explicitly separates the d orbital energies from d–d interelectron repulsion while the DFT orbitals include these effects and within the full molecular symmetry.[26] However, if the molecular potential can be made more spherical, the DFT orbital energies should more closely match those from LFT. An approximate 'spherical' state can be constructed using the ADC concept described above. For a D_{4h} complex, the relevant configuration is $b_{1g}^{1.2}b_{2g}^{1.2}e_g^{2.4}a_{1g}^{1.2}$ corresponding to $d_{x^2-y^2}^{1.2}d_{xy}^{1.2}d_{xz}/d_{yz}^{2.4}d_{z^2}^{1.2}$.

The DFT calculation gives orbitals in the sequence $b_{1g} \ll b_{2g} < e_g < a_{1g}$ with energies relative to $b_{1g}(d_{x^2-y^2})$ of 0, −13711, −18009 and −23259 cm^{-1}. Since b_{2g} is higher than e_g, F^- is predicted to be a π donor. Using these energies in eqns. (6) gives e_σ(F) = 7436 cm^{-1}, e_π(F) = 2149 cm^{-1} and e_{ds}(F) = 2097 cm^{-1}. These values correspond to Δ_{oct} = 13712 cm^{-1}, consistent with the values derived from ligand-field analyses (*vide supra*), and an $e_\pi : e_\sigma$ ratio of 0.29. Using this ratio and maintaining the original Δ_{oct} values based on the r^{-4} dependence yields $e_\sigma = 75652r^{-4}$ cm^{-1} and $e_\pi = 21939r^{-4}$ cm^{-1}.

The variation of the spin state energy term, $E_{spin} = 5B + 8C$, over the bond length range of interest is relatively small (~1 kcal mol^{-1} from 1.88 to 1.97 Å) and does not significantly affect the optimised bond length. The final high-spin LFMM energies is just the sum of E_{str}, E_{vdw} and E_{LFSE} while the final low-spin energy comprises these three terms plus E_{spin}.

To summarise, simple DFT calculations provide three energy curves, one for high spin, one for low spin and one for the hypothetical 'zero LFSE' ADC state. Calculations on planar $[CoF_4]^-$, again using an ADC, give the e_π/e_σ ratio. Together, a set of LFMM parameters can be generated which describes the absolute energies of the high- and low-spin forms of $[CoF_6]^{3-}$ in the gas phase over a wide range of Co–F distances to an uncertainty of about 2 kcal mol^{-1}. The optimal parameters and calculated bond lengths and energies are given in Table 2.

$[Co(CN)_6]^{3-}$

Developing LFMM parameter values for $[Co(CN)_6]^{3-}$ follows virtually the same procedure and the derived parameters and a comparison of observed and calculated data is shown in Table 3. The LDA gives good metal–ligand distances and the predicted value of Δ_{oct} is in excellent agreement with spectroscopic values. The value obtained for r_0 (2.15 Å) corresponds well with the ADC calculation (2.16 Å).

Interestingly, the ADC calculation on hypothetical planar $[Co(CN)_4]^-$ with Co–CN distances of 1.88 Å gives the same d orbital sequence as $[CoF_4]^-$ indicating that cyanide attached to a Co(III) centre is acting as a π donor. However, the computed d orbital energies [−39720, −41865 and −43462 cm^{-1} relative to

Table 3 LFMM parameters for $[Co(CN)_6]^{3-}$ (σ-bonding only) and optimised LFMM bond lengths (Å) and total energies (kcal mol^{-1}). DFT values in italics. D, r_0 and α refer to the Morse function, $\Delta_{oct} = K/r^N$, A and B are the van der Waals parameters and $5B + 8C$ models the d–d interelectron repulsion energy added to the low-spin state

D/kcal mol^{-1}	221.2
r_0/Å	2.152
α	0.69
N	4
K/kcal mol^{-1}	1104
A/kcal mol^{-1} Å^{-9}	14539
B/kcal mol^{-1} Å^{-6}	897
$(5B + 8C)$/kcal mol^{-1}	$-17.84r^2 + 92.44r - 71.77$
Co–CN high spin/Å	4 × 2.12, 2 × 2.11; *2.12*
Total energy, high spin/kcal mol^{-1}	−1357.0; *−1353.8*
Co–CN low spin/Å	1.89; *1.88*
Total energy, low spin/kcal mol^{-1}	−1447.9, *−1448.2*

$b_{1g}(d_{x^2-y^2})$] predict a very much smaller e_π/e_σ ratio of only 0.07. Cyanide has both π donor and π acceptor levels available and the final nature of the π interaction will be a balance. One would expect a high-valent metal centre to have lower energy orbitals and interact more strongly with the filled ligand π orbitals while a low valent centre with higher energy orbitals would favour the ligand π* orbitals. Evidently, the former prevails for Co(III). To maintain the original Δ_{oct} values, $e_\sigma(CN) = 141949r^{-4}$ cm^{-1} and $e_\pi(CN) = 9936r^{-4}$ cm^{-1} which at a Co–CN distance of 1.88 Å yield $\Delta_{oct} = 39721$ cm^{-1} in modest agreement with data derived from ligand field analysis.

Mixed ligand systems

The acid test of the utility of the LFMM method is whether the parameters are transferable. Here, we have used quick and easy DFT calculations to help develop parameters which give a good description of the structures and spin state energies of the homoleptic complexes. Will these same parameters be capable of modelling all the mixed-ligand systems in-between? As a preliminary, we need to know the structures and spin state energies for $[CoF_n(CN)_{6-n}]^{3-}$, n = 1–5. Since to our knowledge, none of these complexes has ever been synthesised and structurally characterised, the entire exercise is forced to rely on DFT. Accordingly, the LDA and BP86 structures were computed for both high- and low-spin forms of all the mixed-ligand systems. The LFMM structures were then compared to the LDA results while the LFMM spin-state energy differences were compared to the BP86 energy differences computed at the BP86 geometries. All relevant data are available as ESI. †

The spin-state energy differences are reasonably well reproduced (Fig. 3). The overall trend of increasing energy difference as F^- ligands are replaced is reproduced as is the energy change within isomeric pairs. That is, both DFT and LFMM predict smaller energy gaps for *trans* and *mer* relative to *cis* and *fac* respectively. The rms deviation is 6.9 kcal mol^{-1} which might seem rather high were it not for the systematic overestimates of the LFMM for mixed-ligand systems plus the increasingly larger magnitudes as the number of CN^- ligands increases. This can be traced to a systematic error in the total LFMM energies for mixed-ligand systems (Fig. 4). Relative to homoleptic complexes, DFT gives larger variations in Co–F and Co–CN bonds for mixed-ligand species than the LFMM, especially for high-spin complexes. Consequently, the DFT energies are always lower than their LFMM counterparts.

Despite these differences, the primary goal is realised. From a treatment of just the homoleptic species, the LFMM correlates well with the DFT spin-state energy differences for all the mixed-ligand systems.

The structures of the mixed-ligand systems are also satisfactory, especially for the low-spin species (Table 4) where the rms deviation between DFT and LFMM is 0.03 Å. Aspects of the

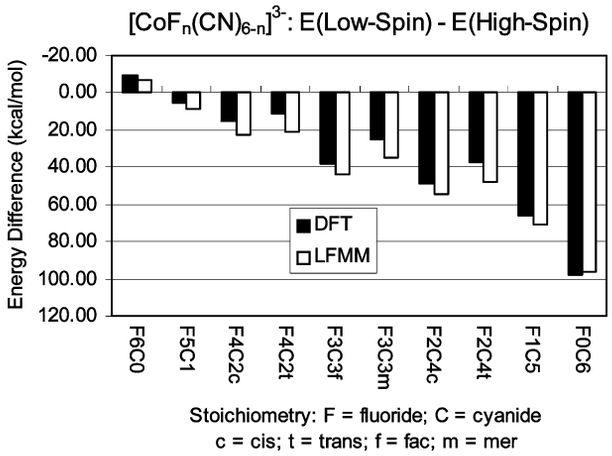

Fig. 3 Comparison of DFT and LFMM spin-state energy differences for the series $[CoF_n(CN)_{6-n}]^{3-}$, n = 0–6.

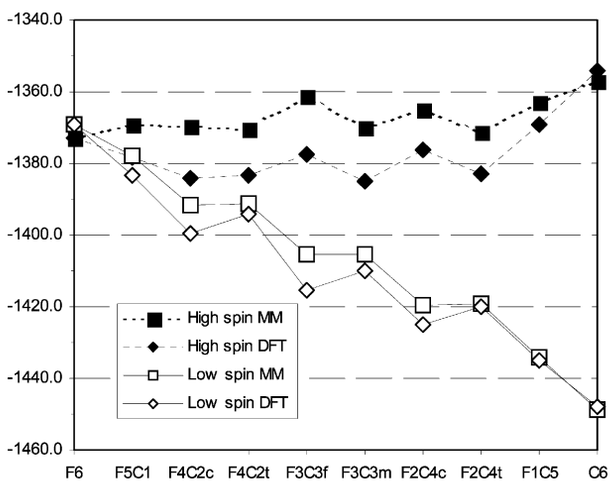

Fig. 4 Comparison of DFT and LFMM total energies.

high-spin structures are more difficult to reproduce (Table 5). In particular, the *cis* and *trans* influences between F^- and CN^- are not fully accounted for. The LFMM gives too short Co–CN contacts, by up to 0.2 Å in the extreme case of high-spin $[CoF_5(CN)]^{3-}$ and too long Co–F distances with the worst error of 0.1 Å for high-spin *trans*-$[CoF_2(CN)_4]^{3-}$. The former implies an error in treating the *trans* influence while the latter, where F and CN are mutually *trans*, suggests some imbalance in the treatment of *cis* effects. This increases the rms error for high-spin species to 0.06 Å. However, the effect on the energies is less pronounced because there is an element of cancellation. Relative to DFT, what the LFMM loses with too long Co–F contacts is partially recovered by giving too short Co–CN distances. The model could presumably be improved by optimising the ligand van der Waals parameters and/or modifying the ligand-field parameters from their standard values to reflect the nature of the groups in the *cis* and *trans* positions. The latter seems intuitively appealing since the interpretation of the *trans* influence, say, as one ligand increasing its bond energy at the expense of the *trans* group could be simulated by suitable modification of e_σ and e_π parameters for each ligand. We are in the process of developing the necessary computer code to implement these ideas in the context of planar d^8 complexes.

Conclusions

This study establishes that an LFMM approach based on parameterising homoleptic systems can successfully reproduce

Table 4 Optimised geometrical data for low-spin systems. Normal text = DFT, italics = LFMM

Complex, symmetry	Co–F/Å	Co–CN/Å	Angle/°
$[CoF_5(CN)]^{3-}$, C_{4v}	F *trans*: 1.87; *1.88* CN *trans*: 1.92; *1.88*	F *trans*: 1.84; *1.91*	F_{ax}–Co–F_{eq}: 89; *90*
cis-$[CoF_4(CN)_2]^{3-}$, C_{2v}	F *trans*: 1.86; *1.88* CN *trans*: 1.90; *1.88*	F *trans*: 1.83; *1.90*	C–Co–C: 92; *90*
trans-$[CoF_4(CN)_2]^{3-}$, D_{4h}	F *trans*: 1.87; *1.88*	CN *trans*: 1.91; *1.91*	
fac-$[CoF_3(CN)_3]^{3-}$, C_{3v}	CN *trans*: 1.89; *1.88*	F *trans*: 1.83; *1.90*	F–Co–F: 89; *90* C–Co–C: 92; *90*
mer-$[CoF_3(CN)_3]^{3-}$, C_{2v}	F *trans*: 1.87; *1.88* CN *trans*: 1.90; *1.88*	F *trans*: 1.83; *1.90* CN *trans*: 1.91; *1.90*	F–Co–F(*cis*): 89; *90* F–Co–C(*cis*): 90; *90*
cis-$[CoF_2(CN)_4]^{3-}$, C_{2v}	CN *trans*: 1.90; *1.88*	F *trans*: 1.83; *1.90* CN *trans*: 1.89; *1.90*	F–Co–F: 89; *90*
trans-$[CoF_2(CN)_4]^{3-}$, D_{4h}	F *trans*: 1.88; *1.88*	CN *trans*: 1.90; *1.90*	
$[CoF(CN)_5]^{3-}$, C_{4v}	CN *trans*: 1.91; *1.88*	F *trans*: 1.83; *1.90* CN *trans*: 1.88; *1.90*	F–Co–C_{eq}: 90; *90*

Table 5 Optimised geometrical data for high-spin systems. Normal text = DFT, italics = LFMM

Complex, DFT symmetry	Co–F/Å	Co–CN/Å	Angle/°
$[CoF_5(CN)]^{3-}$, C_{4v}	F *trans*: 1.92; *1.96* CN *trans*: 1.97; *1.99*	F *trans*: 2.32; *2.12*	F_{ax}–Co–F_{eq}: 92; *91*
cis-$[CoF_4(CN)_2]^{3-}$, C_{2v}	F *trans*: 1.86; *1.93* CN *trans*: 1.95; *1.99*	F *trans*: 2.24; *2.11*	C–Co–C: 94; *89*
trans-$[CoF_4(CN)_2]^{3-}$, D_{4h}	F *trans*: 1.91; *1.96*	CN *trans*: 2.25; *2.11*	
fac-$[CoF_3(CN)_3]^{3-}$, C_{3v}	CN *trans*: 1.91; *1.96*	F *trans*: 2.19; *2.12*	F–Co–F: 93; *100* C–Co–C: 90; *85*
mer-$[CoF_3(CN)_3]^{3-}$, C_{2v}	F *trans*: 1.84; *1.93* CN *trans*: 1.95; *1.99*	F *trans*: 2.21; *2.11* CN *trans*: 2.20; *2.11*	F–Co–F(*cis*): 92; *91* F–Co–C(*cis*): 89; *91*
cis-$[CoF_2(CN)_4]^{3-}$, C_{2v}	CN *trans*: 1.88; *1.94*	F *trans*: 2.16; *2.14* CN *trans*: 2.17; *2.11*	F–Co–F: 91; *134*
trans-$[CoF_2(CN)_4]^{3-}$, D_{4h}	F *trans*: 1.83; *1.93*	CN *trans*: 2.19; *2.11*	
$[CoF(CN)_5]^{3-}$, C_{4v}	CN *trans*: 1.81; *1.92*	F *trans*: 2.13; *2.14* CN *trans*: 2.15; *2.11*	F–Co–C_{eq}: 94; *95*

the structures and energies of all the mixed-ligand species as well. In the present case where experimental data are absent, the LFMM results were compared to those from DFT. LFMM parameters developed from only $[CoF_6]^{3-}$ and $[Co(CN)_6]^{3-}$ work unchanged for the eight mixed-ligand systems giving high-spin and low-spin structures with Co–L rms errors of 0.06 and 0.03 Å, respectively. In addition, explicit recognition of d–d interelectron repulsion energies provides a common reference for both spin states which facilitates a direct LFMM calculation of the spin-state energy difference. The LFMM predicts: (i) a change from high to low spin after replacement of a single fluoride ligand; (ii) the difference increases with each subsequent replacement and (iii) $^1A_{1g}$ is relatively more stable for *cis* and *mer* compared to *trans* and *fac* respectively. The DFT calculations concur.

Although the LFMM FF performs well, there are some areas where further improvements could be made. For example, the *trans* and *cis* influences between F^- and CN^- are not fully captured, especially for the high-spin, Jahn–Teller active species. Compared to DFT, the LFMM gives too long a Co–F distance and too short a Co–CN bond. Fortunately, this does not have serious consequences for the energy estimates since the errors tend to cancel. Nevertheless, the *trans* and *cis* influences are widespread phenomena and we are examining strategies for a better treatment within the LFMM scheme.

In conclusion, as a 'proof of concept', it has been a valuable exercise to show that the LFMM can be designed to simulate results from far more sophisticated and computationally demanding DFT calculations. The results reported here give us the confidence to extend the LFMM parameterisation to the condensed phase, in particular, aqueous solution. This should also allow us to treat a far wider range of metal–ligand combinations in complexes with different overall charges. Results for Fe(II) and Fe(III) species will be reported in due course.

Acknowledgements

The authors thank the EPSRC for a project studentship (B. J. W. H.) and a postdoctoral fellowship (D. L. F.) and for provision of computing facilities *via* a JREI equipment grant.

References

1 B. R. Brooks, R. E. Bruccoleri, B. D. Olafson, D. J. States, S. Swaminathan and M. Karplus, *J. Comput. Chem.*, 1983, **4**, 187.
2 T. A. Halgren, *J. Comput. Chem.*, 1996, **17**, 553.
3 D. A. Pearlman, D. A. Case, J. W. Caldwell, W. S. Ross, T. E. Cheatham, S. Debolt, D. Ferguson, G. Seibel and P. Kollman, *Comput. Phys. Commun.*, 1995, **91**, 1.
4 P. Comba and T. W. Hambley, *Molecular Modeling of Inorganic Compounds*, VCH, New York, 1995.
5 R. J. Deeth, *Coord. Chem. Rev.*, 2001, **212**, 11.
6 P. Comba and M. Zimmer, *J. Chem. Educ.*, 1996, **73**, 108.
7 R. D. Hancock, *Prog. Inorg. Chem.*, 1989, **37**, 187.
8 V. S. Allured, C. M. Kelly and C. R. Landis, *J. Am. Chem. Soc.*, 1991, **113**, 1.
9 V. J. Burton, R. J. Deeth, C. M. Kemp and P. J. Gilbert, *J. Am. Chem. Soc.*, 1995, **117**, 8407.
10 R. J. Deeth and V. J. Paget, *J. Chem. Soc., Dalton Trans.*, 1997, 537.
11 R. J. Deeth and D. L. Foulis, *Phys. Chem. Chem. Phys.*, 2002, **4**, 4292.
12 ADF version 2.3.0, Theoretical Chemistry, Vrije Universiteit', Amsterdam, 1997.
13 ADF 2000.01, E. J. Baerends, A. Bérces, C. Bo, P. M. Boerrigter, L. Cavallo, L. Deng, R. M. Dickson, D. E. Ellis, L. Fan, T. H. Fischer, C. Fonseca Guerra, S. J. A. van Gisbergen, J. A. Groeneveld, O. V. Gritsenko, F. E. Harris, P. van den Hoek, H. Jacobsen, G. van Kessel, F. Kootstra, E. van Lenthe, V. P. Osinga, P. H. T. Philipsen, D. Post, C. C. Pye, W. Ravenek, P. Ros, P. R. T. Schipper, G. Schreckenbach, J. G. Snijders, M. Sola, D. Swerhone, G. te Velde, P. Vernooijs, L. Versluis, O. Visser, E. van Wezenbeek, G. Wiesenekker, S. K. Wolff, T. K. Woo and T. Ziegler, 2000.

14 E. J. Baerends, D. E. Ellis and P. Ros, *Theor. Chim. Acta*, 1972, **27**, 339.
15 J. C. Slater, *Adv. Quantum Chem.*, 1972, **6**, 1.
16 S. H. Vosko, L. Wilk and M. Nusair, *Can. J. Phys.*, 1980, **58**, 1200.
17 A. D. Becke, *Phys. Rev. A*, 1988, **38**, 3098.
18 J. P. Perdew and W. Yue, *Phys. Rev. B: Condens. Matter*, 1986, **33**, 8800.
19 J. P. Perdew, *Phys. Rev. B: Condens. Matter*, 1988, **37**, 4267.
20 CAMMAG, D. A. Cruse, J. E. Davies, M. Gerloch, J. H. Harding, D. J. Mackey and R. F. McMeeking, Cambridge, 1983.
21 M. R. Bray, R. J. Deeth, V. J. Paget and P. D. Sheen, *Int. J. Quantum Chem.*, 1997, **61**, 85.
22 B. N. Figgis and M. A. Hitchman, *Ligand Field Theory, and Its Applications*, John Wiley and Sons Ltd., New York, 2000.
23 G. C. Allen, G. A. M. El-Sharkawy and K. D. Warren, *Inorg. Chem.*, 1971, **10**, 2538.
24 L. G. Vanquickenborne, K. Pierloot and E. Duyvejonck, *Chem. Phys. Lett.*, 1994, **224**, 207.
25 J. C. Slater, *The Self-consistent Field for Molecules and Solids*, McGraw-Hill, London, 1974.
26 R. J. Deeth, *Faraday Discuss.*, 2003, **124**, 379.